Journal of Controlled Release 330 (2021) 788–796

Contents lists available at ScienceDirect

Journal of Controlled Release

journal homepage: www.elsevier.com/locate/jconrel

Self-assembling A6K peptide nanotubes as a mercaptoundecahydrododecaborate (BSH) delivery system for boron neutron capture therapy (BNCT)

Hiroyuki Michiue [a,*], Mizuki Kitamatsu [b], Asami Fukunaga [c], Nobushige Tsuboi [d], Atsushi Fujimura [c], Hiroaki Matsushita [c], Kazuyo Igawa [a], Tomonari Kasai [a], Natsuko Kondo [e], Hideki Matsui [a,c], Shuichi Furuya [a]

[a] Neutron Therapy Research Center, Okayama University, Japan
[b] Department of Applied Chemistry, Kindai University, Japan
[c] Department of Physiology, Okayama University Graduate School of Medicine, Dentistry and Pharmaceutical Sciences, Okayama, Japan
[d] Department of Neurological Surgery, Okayama University Graduate School of Medicine, Dentistry, and Pharmaceutical Sciences, Okayama, Japan
[e] Institute for Integrated Radiation and Nuclear Science, Kyoto University, Japan

ARTICLE INFO

Keywords:
Malignant brain tumor
Boron neutron capture therapy (BNCT)
Peptide nanotube
Boron drug
Drug delivery system (DDS)
A6K peptide

ABSTRACT

Boron neutron capture therapy (BNCT) is a tumor selective therapy, the effectiveness of which depends on sufficient ^{10}B delivery to and accumulation in tumors. In this study, we used self-assembling A6K peptide nanotubes as boron carriers and prepared new boron agents by simple mixing of A6K and BSH. BSH has been used to treat malignant glioma patients in clinical trials and its drug safety and availability have been confirmed; however, its contribution to BNCT efficacy is low. A6K nanotube delivery improved two major limitations of BSH, including absence of intracellular transduction and non-specific drug delivery to tumor tissue. Varying the A6K peptide and BSH mixture ratio produced materials with different morphologies—determined by electron microscopy—and intracellular transduction efficiencies. We investigated the A6K/BSH 1:10 mixture ratio and found high intracellular boron uptake with no toxicity. Microscopy observation showed intracellular localization of A6K/BSH in the perinuclear region and endosome in human glioma cells. The intracellular boron concentration using A6K/BSH was almost 10 times higher than that of BSH. The systematic administration of A6K/BSH *via* mouse tail vein showed tumor specific accumulation in a mouse brain tumor model with immunohistochemistry and pharmacokinetic study. Neutron irradiation of glioma cells treated with A6K/BSH showed the inhibition of cell proliferation in a colony formation assay. Boron delivery using A6K peptide provides a unique and simple strategy for next generation BNCT drugs.

1. Introduction

Current advanced cancer therapy includes surgery, chemotherapy, and radiation therapy; however, glioblastoma multiforme (GBM) remains the most treatment-resistant malignant primary brain tumor, with a median survival of approximately 1.5 years [1]. Most anti-cancer drugs—including molecular targeted drugs—used in the treatment of various cancers are ineffective for GBM owing to the presence of the blood–brain barrier and various other brain specific challenges [2]. Therefore, the development of novel anti-GBM treatments with combined drug and radiotherapy is a promising approach for treatment for GBM after surgery, particularly for elderly patients [3]. Boron neutron capture therapy (BNCT) is one of the most promising GBM treatments. BNCT is based on the neutron capture and fission reactions that ^{10}B atoms undergo with low-energy neutrons on the irradiation of brain tumor tissues with thermal or epithermal neutron beams [4]. The BNCT reaction involves high-energy transfer alpha particles (^{4}He) and ^{7}Li nuclei with particle ranges that are approximately within the size of the cell diameter (<10 μm) [5]. Upon neutron irradiation, only GBM cells containing ^{10}B are killed by the boron neutron reaction, while the surrounding normal cells remain unaffected. BNCT is therefore an ideal cell-targeting radiotherapy [6]. BNCT has been applied to several

* Corresponding author at: Neutron Therapy Research Center, Okayama University, 2-5-1 Shikata-cho, Kita-ku, Okayama 700-8558, Japan.
E-mail address: hmichiue@md.okayama-u.ac.jp (H. Michiue).

https://doi.org/10.1016/j.jconrel.2020.11.001
Received 25 May 2020; Received in revised form 25 October 2020; Accepted 1 November 2020
Available online 11 November 2020

obstinate malignancies including GBM, head and neck cancer, melanoma, hepatic cancers, and lung cancers, among others [7]. The therapeutic efficacy of BNCT depends on the tumor specific boron uptake and abundant neutron irradiation of the tumor area [8,9]. Recently, the neutron source used for BNCT has been changed to an accelerated neutron source that can be installed in hospitals, which eliminates the need for a reactor neutron source [10]. One of the greatest challenges in BNCT has been developing new boron drugs for application to several malignant tumors—in addition to BPA [11]. BPA (4-borono-*L*-phenylalanine) is the leading BNCT boron drug for treating malignant melanoma and is based on an amino acid analogue fused boron. Many researchers have reported that L-amino acid transporter-1 (LAT-1)—expressed in many malignant tumor cell lines and cancer tissues—imports BPA into malignant tumor cells [12,13]. BSH (disodium undecahydro-mercapto-closo-dodecacarborate) has been used in combination with BPA for treatment of primary malignant glioma BNCT [14] and the combination led to significantly longer survival outcomes compared with those for BNCT with BPA only [15]. BPA is of course a leading player in BNCT, however a limitation of BPA is that the expression of LAT-1 in cancer tissue is non-uniform and the intracellular uptake of BPA is inhomogeneous. Therefore, new boron drugs with different intracellular uptake pathways for combined use with BPA are essential for developing BNCT efficacy [16].

Drug delivery systems (DDS) for boron agents, including polymeric macromolecule DDS such as liposomes and emulsions, which combine BSH and several boron compounds, are interesting and adaptable tools in preclinical BNCT experiments [17]. In this work, we focused on a peptide DDS using A6K peptide [18]. A6K comprises six alanine residues and one lysine (AAAAAAK) and has been reported as an siRNA (small interfering RNA) delivery tool [19]. In this work we aimed to demonstrate a new boron delivery system based on A6K peptide and BSH, and open up a novel direction for boron agents in the next generation of BNCT.

2. Materials and methods

2.1. A6K peptide, boron cluster (BSH), and preparing the A6K/BSH complex

BSH was purchased from KATCHEM (Czech Republic) and A6K peptide was kindly provided by 3-D Matrix, Ltd. (Tokyo, Japan). A 10 mM solution of A6K was prepared in sterilized Milli-Q water using ultrasound sonication. 2 M BSH solution was used to prepare different ratio mixtures with A6K peptide.

2.2. Scanning electron microscopy and sample preparation

A6K/BSH complex mixtures; 1:1 (20 μM A6K/20 μM BSH), 1:2.5 (20 μM A6K/50 μM BSH, 1:5 (20 μM A6K/100 μM BSH), 1:10 (20 μM A6K/200 μM BSH), 1:20 (20 μM A6K/400 μM BSH), and 1:50 (20 μM A6K/1 mM BSH) were placed on cover glass (Fisherbrand microscope cover glass 18CIRCLE) and allowed to dry naturally on the scanning electron microscope (SEM) stage. All samples were observed using SEM at the following magnifications; 10,000, 40,000, 80,000, and 200,000 (S-4800, Hitachi Power Solutions Co. Ltd). The average diameter of the nano-complex was calculated from a total of 50 particles in different observation fields.

2.3. Cell culture of human glioma cell line

A human malignant glioma cell line—U87 delta EGFR glioma cell line, kindly provided by Prof. W. Cavenee and Dr. A. Mukasa (Department of Cellular & Molecular Medicine, University of California, San Diego, CA, USA)—which stably expresses constitutively active EGFRvIII, was used in all experiments. The cells were maintained in Dulbecco's modified Eagle's medium (DMEM; Wako) with 10% fetal bovine serum (FBS), penicillin, and streptomycin at 37 °C in a humidified atmosphere containing 5% CO_2.

2.4. Cell proliferation assay (WST-1 assay)

After the glioma cells (1×10 [3]/well) were seeded in 96-well flat-bottomed plates, they were cultured in DMEM containing 10% FBS for 24 h. The cells were then supplemented with different concentrations of either A6K/BSH, or A6K peptide, and incubated for a further 24 h. Cell viability was measured using the WST-1 (Water-Soluble Tetrazolium) assay according to the manufacturer's instructions (Roche Applied Science).

2.5. Inductively coupled plasma (ICP) measurement of intra-cellular boron

All of the cell samples were measured by ICP (ICP-AES, VISTA-PRO, Seiko Instruments Inc.) using a previously described method [9]. The intracellular boron concentration (^{10}B ng/10^6 cells) was calculated from the amount of boron present and the cell number of the sample. The ICP measurement was overseen by Dr. H. Nagare (Okayama University Faculty of Environmental Science and Technology).

2.6. Immunocytochemistry (ICC) of human glioma cells

ICC was performed to analyze the distribution of BSH *in vitro*. The anti-BSH mouse antibody was kindly provided by Prof M. Kirihata, Osaka Prefectural University. The early endosome marker (CellLight™ Early Endosomes-RFP, BacMam 2.0, Thermo Fisher Scientific) was used in accordance with the manufacturer's instructions. The cells were cultured on poly-L-lysine coated cover glass (4912–040, IWAKI) with BSH or A6K/BSH complex for 0.5, 6, 12, and 24 h. After incubation with the boron compounds, the cells were thoroughly washed five times with PBS, fixed with 4% paraformaldehyde (PFA) for 30 min, and incubated with mouse anti-BSH mAb. The secondary antibody was incubated with mouse IgG conjugated Alexa-Fluor 488 for 2 h. Nuclear staining with Hoechst 33258 and cytoplasmic staining with Phalloidin 555 were carried out for 30 min, and intracellular fluorescence signals were observed using a confocal laser microscope (FV1200, Olympus, Japan).

2.7. Mouse brain tumor model with immunohistochemistry (IHC) and pharmacokinetics (PK)

All animal use and care procedures were approved by the Department of Animal Resources, Advanced Science Research Center, Okayama University (OKU-2016475, OKU-2019091) and followed all required protocols. Athymic mice were used (BALB/C-nu/nu, female, 6–8 weeks, 16–20 g, Japan SLC, Inc.). After two weeks, BSH (20 mM) or A6K/BSH complex (2 mM A6K/20 mM BSH), 10 μL/g (mouse body weight), were injected intravenously through the tail vein of the tumor-bearing mice for IHC. 12 h after injection, the mice were euthanized, and the brains were resected and placed in 10% PFA. Brain sections of 10 μm thickness were cut on a microtome (CM 1850; Leica Microsystems, Wetzlar, Germany). The IHC was carried out with 4% PFA fixing, 1% (w/v) BSA blocking; primary antibodies, anti-BSH antibody—kindly provided by Prof. M. Kirihata (Research Center for Boron Neutron Capture Therapy, Osaka Prefecture University)—and HLA-A; Secondary antibodies, anti-mouse IgG fused Alexa-Fluor 488 and anti-rabbit IgG fused Alexa-Fluor 555; and nuclear staining was achieved with Hoechst 33258. All of the samples were observed using a confocal laser microscope (FV1200, Olympus, Japan).

In PK, A6K/BSH complex (2 mM A6K/20 mM BSH), 50 mg/kg (BSH/mouse body weight), were injected intravenously through the tail vein of the brain tumor-bearing mice. 1 h, 2 h, and 24 h after injection, the mice were euthanized, each organ (heart, lung, brain, kidney, liver, blood, and brain tumor) was resected. And all samples were measured

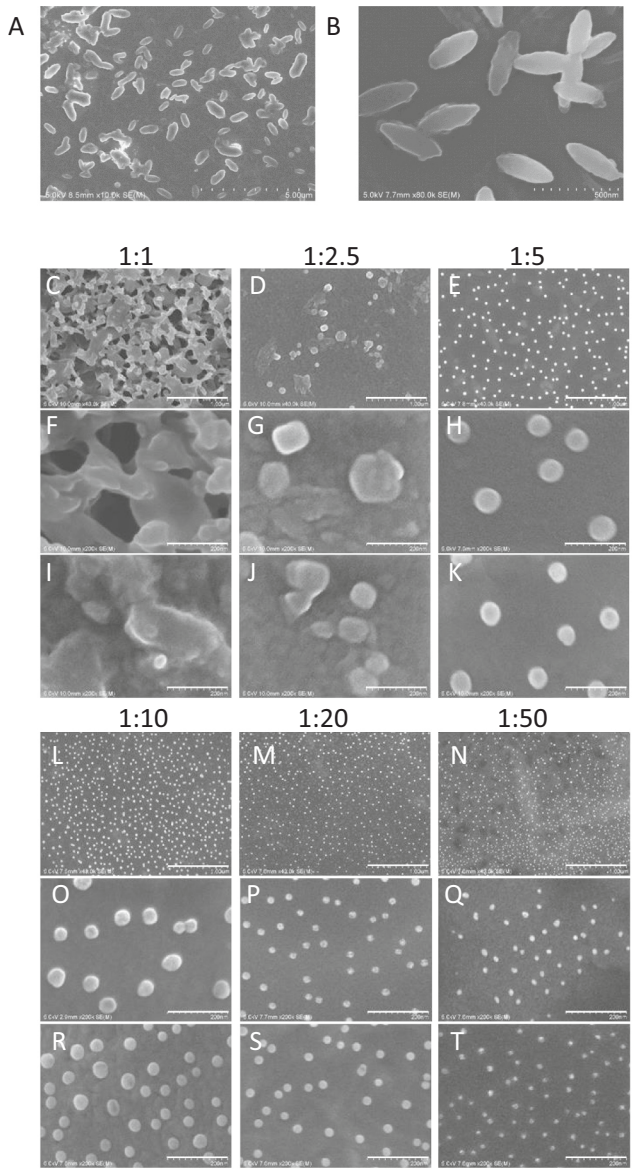

Fig. 1. Scanning electron microscopy imaging of A6K peptide nanotubes and different mixture ratios of A6K/BSH complex: (A), (B) SEM images of A6K peptide nanotubes, magnification ratio (A) ×10,000, (B) ×80,000. (C)–(T) SEM images of A6K/BSH complexes with different mixture ratios of A6K and BSH. The upper rows (1-C, D, E, L, M, N) for the A6K/BSH complexes show low magnification ×40,000 images and the middle and lower rows (1-F, G, H, I, J, K, O, P, Q, R, S, T) show high magnification ×200,000 images.

the weight, completely dissolved with 60% nitric acids and heat treatment, and determined boron concentration with ICP-MS (Agilent technologies 7500cx, USA) in Institute of Plant Science and Resources (IPSR), Okayama University, Japan.

2.8. Neutron radiation experiment at the Institute for Integrated Radiation and Nuclear Science, Kyoto University (KURNS)

All protocols were approved by the KURNS ethics committee. 24 h before neutron irradiation, the U87 delta EGFR cell line was treated with 200 μM A6K/2 mM BSH (final concentrations) or 100 μM A6K/1 mM BSH (final concentrations). Just before neutron irradiation, the cell samples were transferred to collecting tubes and subjected to 1 MW neutron irradiation (thermal neutron flux 1.4×10^{9} neutron/cm^2/s) for 5 min (thermal neutron fluence 4.4×10^{11} neutron/cm^2, γ-ray 0.7 × 10^{-1} Gy), 15 min (thermal neutron fluence 1.1×10^{12} neutron/cm^2, γ-ray 1.7×10^{-1} Gy), or 30 min (thermal neutron fluence 2.8×10^{12} neutron/cm^2, γ-ray 3.1×10^{-1} Gy) (Fig. 5A, C, D). In addition, U87 delta EGFR were treated with 2 mM BSH; 200 μM A6K/2 mM BSH; or 100 μM A6K/1 mM BSH (final concentrations) and subjected to 1 MW neutron irradiation at the KURNS facility for 15 min (thermal neutron fluence 1.1×10^{12} neutron/cm^2, γ-ray 2.5×10^{-1} Gy) and 30 min (thermal neutron fluence 2.4×10^{12} neutron/cm^2, γ-ray 5.5×10^{-1} Gy). After irradiation, all glioma cells were re-cultured in 96 well plates (9×10^{3} cells/well) for 24 h and 48 h, and cell proliferation was measured with Cell Proliferation Reagent WST-1 (Roche, Basel) using a microplate reader (Vient XS, DS Pharma Promo Co., Ltd) (Fig. 5B). A colony formation assay was carried out after 2 weeks of culture with U87 delta EGFR in 60 mm culture dishes (n = 4) and all culture cells were stained with 0.5% Crystal Violet (CV) in 20% methanol. The colonies of CV stained samples were counted automatically with an aCOLyte 3 automatic colony counter machine, (Synbiosis, A Division of Synoptics Ltd) and all data were statistically analyzed.

Table 1
List of average particle diameters measured from SEM images (in each case n = 50 ± SD).

A6K/BSH mixture ratio	Average particle diameter (nm) n = 50
1:1	Impossible to measure
1:2.5	132.6 ± 25.4
1:5	73.7 ± 19.9
1:10	39.3 ± 17.4
1:20	24.5 ± 3.6
1:50	18.3 ± 2.5
A6K peptide nanotube	Long diameter 522.5 ± 92.2 Short diameter 229.4 ± 43.9

2.9. Zeta potential measurement

All A6k (0.1 mM, 0.2 mM, and 0.4 mM) and A6K/BSH (0.1 mM/1.0 mM, 0.2 mM/2.0 mM, and 0.4 mM/4.0 mM) samples were measured using a Zetasizer Nano ZSP (N = 9) in accordance with the manufacturer's instructions (Malvern Panalytical).

2.10. Statistical analysis

All data are presented as mean ± standard error of the mean (SEM). The data were analyzed for statistical significance using Student's *t*-test. Difference was assessed with a two-side test with an alpha level of 0.05. A statistically significant difference was defined as $p < 0.05$.

3. Results

3.1. Scanning electron microscopy images and zeta potential of A6K and A6K/BSH complexes

A6K peptide nanotubes (20 μM) in Milli-Q water were placed on a cover glass on an SEM stage and allowed to dry naturally at room temperature before osmium evaporation coating. The SEM image of A6K peptide nanotubes showed self-assembled tube shapes and with an average long dimension of 522.5 ± 92.2 nm and average short dimension of 229.4 ± 43.9 nm (Fig. 1A, B, Table 1). The magnifying power used to acquire the SEM images in Fig. 1C, D, E, L, M, and N was 40,000 and that for Fig. 1F, G, H, I, J, K, O, P, Q, R, S, and T was 200,000. The 1:1 mixture ratio of A6K/BSH (20 μM A6K/20 μM BSH) did not show individual particles, but continuous dendritic materials (Fig. 1C, F, I), and particle size measurement was not possible (Table 1). The 1:2.5 mixture complex (20 μM A6K/50 μM BSH) showed irregular particles of various sizes and the average diameter was 132.6 ± 25.4 nm (Fig. 1D, G, J, Table 1). The mixture ratios 1:5 (20 μM A6K/100 μM BSH), 1:10 (20

Table 2
List of average zeta potential values measured using a Zetasizer Nano ZSP (in each case n = 9 ± SD).

A6K (mM)	0.1	0.2	0.4
Zeta potential (mV)	+42.6 ± 2.7	+48.2 ± 2.4	+50.4 ± 1.6
A6K/BSH (mM) mixture ratio 1:10	0.1/1.0	0.2/2.0	0.4/4.0
Zeta potential (mV)	−38.2 ± 1.9	−39.6 ± 2.0	−41.3 ± 1.4

μM A6K/200 μM BSH), 1:20 (20 μM A6K/400 μM BSH), and 1:50 (20 μM A6K/1 mM BSH) showed spherical particles in the SEM images and the particle diameters were measured to be 18.3–73.7 nm from the SEM images acquired using a simple drying method (Fig. 1E, H, K, L, M, N, O, P, Q, R, S, T, Table 1). Altering the mixture molar ratio of A6K and BSH resulted in different particle shapes and sizes in the SEM images. The zeta potential of different concentrations of A6K or A6K/BSH was measured using a Zetasizer Nano ZSP. All A6K samples showed positive zeta potentials (0.1 mM A6K: +42.6 ± 2.7 mV, 0.2 mM A6K: +48.2 ± 2.4 mV, 0.4 mM A6K: +50.4 ± 1.6 mV). In contrast, all A6K/BSH showed negative zeta potentials (0.1 mM A6K/1.0 mM BSH: −38.2 ± 1.9 mV, 0.2 mM A6K/2.0 mM BSH: −39.6 ± 2.0 mV, 0.4 mM A6K/4.0 mM BSH: −41.3 ± 1.4 mV) (Table 2).

3.2. Optimization of the mixture ratio of A6K/BSH through evaluation of intracellular boron concentration in human glioma cells

Optimization of the A6K/BSH ratio is essential for boron drug delivery systems using A6K peptide nanotubes. BSH and A6K peptide were mixed in a tube by gentle pipetting and administered to the glioma culture medium. Initially, the BSH concentration was fixed a1t 2 mM in the final medium concentration, and the A6K concentration was varied to 20, 100, 200, and 400 μM in the final concentration—mixture ratios of A6K/BSH of 1:100, 5:100 (1:20), 10:100 (1:10), and 20:100 (1:5),

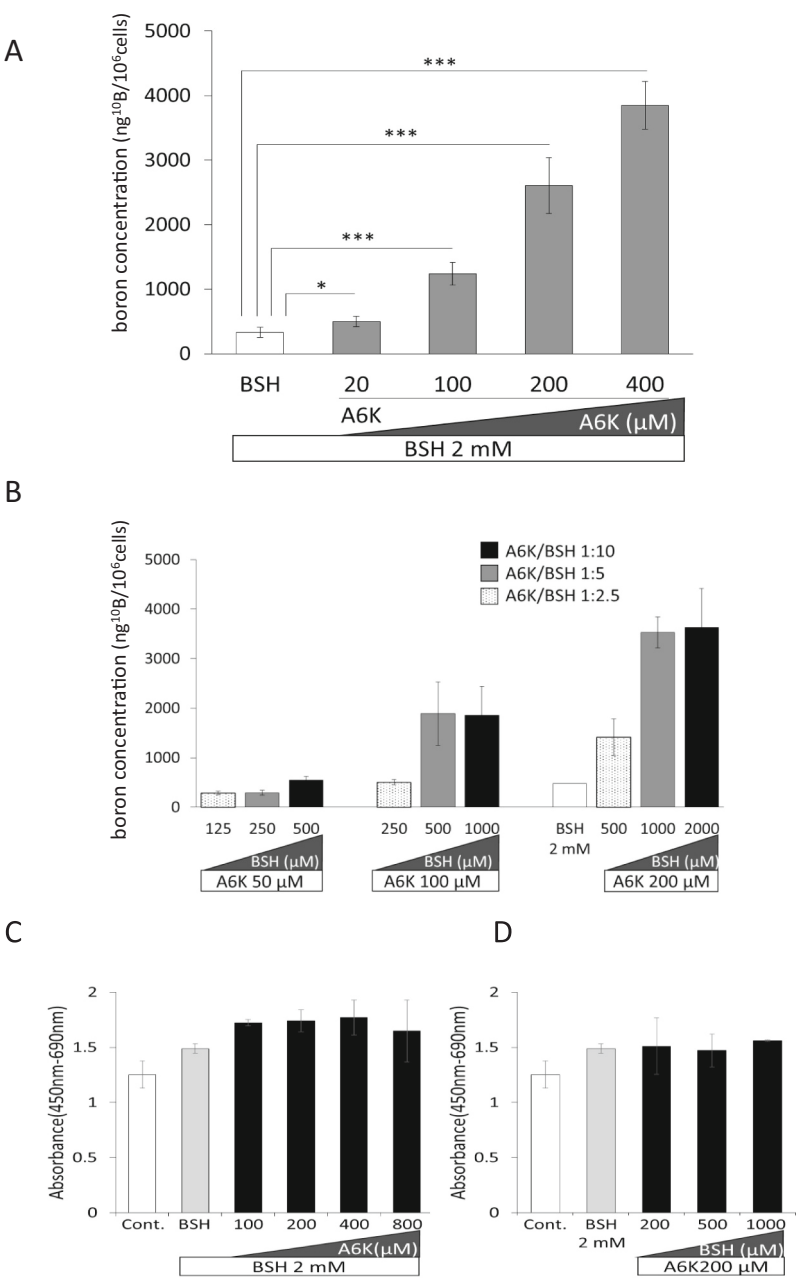

Fig. 2. Intracellular boron concentration and cytotoxicity of different mixture ratios of A6K and BSH incubated with U87 delta EGFR cells for 24 h: (A), (B) Human glioma cells were treated with BSH only or different A6K/BSH mixtures. Y-axis shows intracellular boron concentration [ng^{10}B/10^6 cells]. (A) The A6K/BSH ratio was altered to give different mixtures with a fixed 2 mM BSH concentration. (B) The A6K/BSH ratio was altered to give different mixtures with fixed A6K concentrations (50 μM, 100 μM, and 200 μM). (C), (D) WST-1 cell proliferation assay showing boron drug toxicity with different A6K/BSH mixture ratios after 24 h incubation. The mixture ratio was designed with constant BSH or A6K concentration. Y-axis shows the value of absorbance in the range 450–690 nm measured with an absorptiometer.

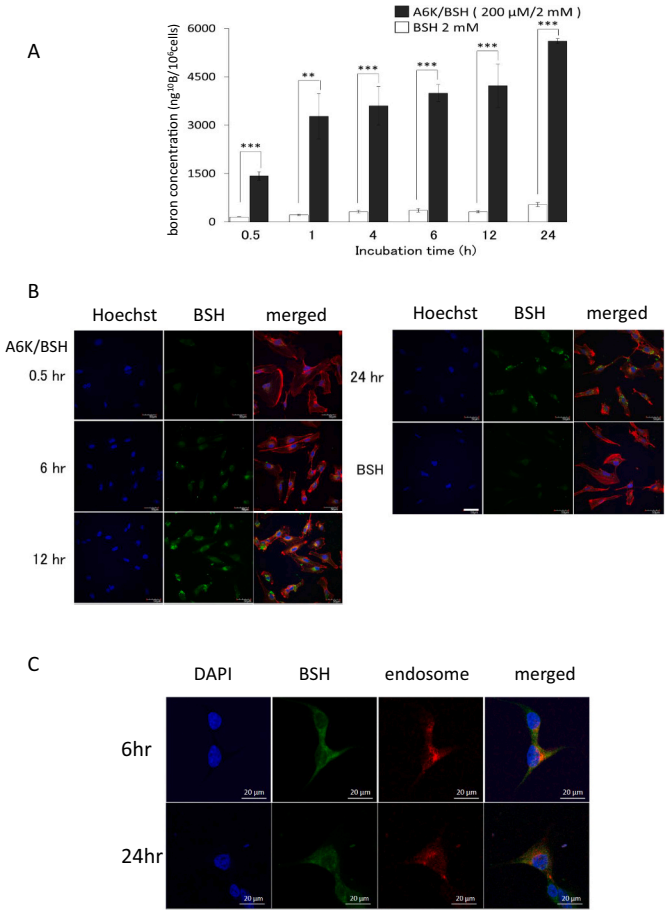

Fig. 3. The intracellular boron concentration and boron localization with complex A6K (200 μM)/BSH (2 mM) over time: (A) Comparison of BSH with the A6K/BSH complex for different incubation times (0.5, 1, 4, 6, 12, and 24 h). Y-axis shows the intracellular boron concentration [ng^{10}B/10^6 cells]. (B) Confocal laser microscopy images of intracellular localization of BSH in human glioma cells over time (0.5, 6, 12, and 24 h). The red signal is F-actin labeled with 555 phalloidin, the green signal is BSH labeled with BSH antibody, and the blue signal is nuclei labeled with Hoechst 33258. (C) Intracellular co-localization of BSH and the endosome in U87 delta EGFR cells using endosome marker (CellLight™ Early Endosomes-RFP) in 6 and 24 h. (For interpretation of the references to colour in this figure legend, the reader is referred to the web version of this article.)

respectively. The most effective intracellular transduction ratio was determined by measurement of the intracellular boron concentration of U87 delta EGFR using ICP-AES. BSH alone was used as a negative control drug that was unable to penetrate cells. The ICP results for different mixture ratios of A6K/BSH from 1:100 to 1:5 administered to glioma cells, showed 498.9 ± 75.1, 1239.9 ± 177.3, 2606.7 ± 430.0, and 3846.4 ± 372.6 [ng^{10}B/10^6 cells] following 24 h culture incubation, respectively (Fig. 2A). Analysis of the mixture ratios 1:2.5, 1:5, and 1:10 with A6K concentrations of 50, 100, and 200 μM showed only small differences between the results for 1:5 and 1:10 (Fig. 2B).

3.3. Cytotoxicity of the A6K/BSH complex determined by cell proliferation assay

All of the complexes were prepared using final concentrations of BSH of 2 mM or 200 μM with different A6K peptide concentrations and the cell proliferation was measured using the WST-1 assay in U87 delta EGFR cells (Fig. 2C, D). Following incubation with the boron complex for 24 h, the absorbance in the range 450–690 nm was measured in 96 well plates following the manufacturer's instructions (Roche Applied Science). None of the A6K/BSH complex treated groups showed any difference in cell proliferation to the control group (Fig. 2C, D). The A6K/BSH boron drug showed no toxicity after 24 h incubation with U87 delta EGFR cells.

3.4. Intracellular boron concentration over time following administration of A6K/BSH complex and immunocytochemistry imaging of BSH localization

The intracellular boron concentration of U87 delta EGFR cells was measured by ICP-AES, and the final medium concentration of each boron drug was 2 mM BSH or 200 μM A6K/2 mM BSH complex. Each sample was analyzed for boron concentration 0.5, 1, 4, 6, 12, and 24 h after continuous incubation (Fig. 3A). The A6K/BSH group showed significantly higher intracellular boron concentration (1425.2 ± 131.5 [ng^{10}B/10^6 cells]) than that of the BSH group (155.7 ± 7.1 [ng^{10}B/10^6 cells]) 0.5 h after sample administration. Following 1, 4, 6, 12, and 24 h of incubation with A6K/BSH cells showed 3272.6 ± 699.4, 3601.3 ± 598.9, 3995.8 ± 263.0, 4223.2 ± 679.9, and 5604.9 ± 78.1 [ng ^{10}B/10^6 cells] and those incubated with BSH showed 218.8 ± 19.0, 318.3 ± 46.5, 358.5 ± 56.6, 318.0 ± 34.4, and 536.0 ± 61.7 [ng ^{10}B/10^6 cells], respectively. The A6K/BSH group showed approximately 10–15 times higher boron concentrations in U87 delta EGFR glioma cells over the time course. We subsequently observed intracellular BSH localization by immunocytochemistry with BSH antibody (green), phalloidin (f-actin, red), and Hoechst (nuclear marker, blue) after administration of the boron agents for 0.5, 6, 12, and 24 h. In the 6 h A6K/BSH group, BSH was observed in the cytoplasmic region and in the 12 and 24 h groups, the BSH signal was clearly seen in the cell and observed particularly strongly in the perinuclear region (Fig. 3B).

To evaluate the cytoplasmic localization with A6K/BSH complex in the 24 h group, early endosome marker (CellLight™ Early Endosomes-RFP, BacMam 2.0, Thermo Fisher Scientific), BSH antibody, and nuclear staining were used (Fig. 3C). The acquired image shows that BSH localized in endosomes after transduction into cells. All of the data indicated the intracellular transduction of A6K/BSH through endocytosis.

3.5. Immunohistochemistry observation and pharmacokinetic study with A6K/BSH complex administration in a mouse brain tumor model

The mouse brain tumor model was established using U87 delta EGFR cells over a 2-week period. In IHC, mice were administered A6K/BSH complex (A6K 2 mM/BSH 20 mM in MilliQ water, 10 μL/mouse body weight [g]) through the tail vein. 12 h after injection, mice were euthanized, a brain tumor sample was taken and the BSH localization *in vivo* was evaluated using immunohistochemistry. Under low magnification (×10), A6K/BSH was observed in the tumor area and peripheral tumor area. In contrast, the brain of the mouse administered BSH alone showed no BSH signal in the normal tissue or tumor areas. At high magnification (×40), the A6K/BSH group showed BSH localized at the tumor core and tumor edge area, but not in normal brain tissue. In PK study, In PK, A6K/BSH complex (50 mg/kg, BSH/mouse body weight), were injected intravenously through the tail vein of the brain tumor-bearing mice. In 1 h, 2 h, and 24 h after injection, each organ (heart, lung, brain, kidney, liver, blood, and brain tumor) was measured boron concentration with ICP-MS (Fig. 4D). The boron concentration in brain tumor reached resected 19.7, 24.8, and 8.9 μg ^{10}B/tissue g, in 1 h, 2 h, and 24 h (Fig. 4D). The brain tumor/normal brain (T/N) ratio was 6.8, 2.8 and 40 (Fig. 4D). These data showed that A6K/BSH accumulated in the tumor and peripheral tumor area as a result of the complexation.

3.6. The boron neutron reaction using neutron irradiation at KURNS

We evaluated the *in vitro* cell killing effect of the boron neutron reaction at the Institute for Integrated Radiation and Nuclear Science,

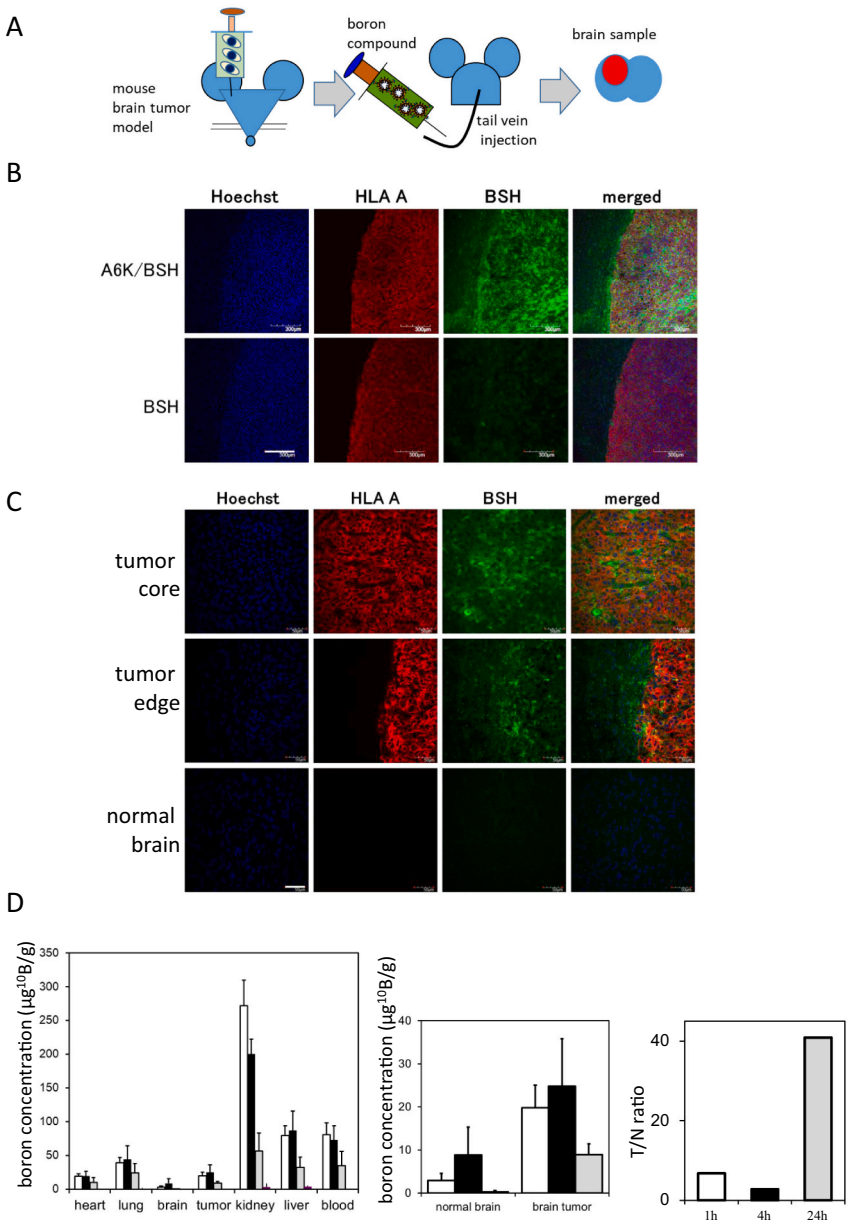

Fig. 4. The systemic administration of A6K/BSH complex in a mouse brain tumor model for IHC and PK: (A) Schematic illustration of boron drug systemic administration through mouse tail vein for treating a mouse brain tumor model. (B)(C) The immunohistochemistry imaging of mouse brain tumor model samples 12 h after mouse tail vein injection of BSH (20 mM) or A6K/BSH complex (2 mM A6K/20 mM BSH), 10 μL/g (mouse body weight). The red signal is anti-human HLA-A antibody, the green signal is BSH labeled with BSH antibody, and the blue signal is nuclei labeled with Hoechst 33258. Scale bars; (B) 300 μm and (C) 50 μm. (D) The pharmacokinetic (PK) study with mouse brain tumor model in 1 h, 2 h and 24 h with mouse tail vein injection of A6K/BSH complex (2 mM A6K/20 mM BSH), 50 mg/kg (BSH /mouse body weight). Tissue ^{10}B concentration (μg^{10}B/tissue g) of all samples measured by ICP-MS. (For interpretation of the references to colour in this figure legend, the reader is referred to the web version of this article.)

Kyoto University (KURNS). The U87 delta EGFR cell line was treated with 100 μM A6K/1 mM BSH or 200 μM A6K/2 mM BSH 24 h before neutron irradiation. Following 1 MW neutron irradiation for 5 min (thermal neutron fluence 4.4×10^{11} neutron/cm^2, γ-ray 0.7×10^{-1} Gy), 15 min (thermal neutron fluence 1.1×10^{12} neutron/cm^2, γ-ray 1.7×10^{-1} Gy), and 30 min (thermal neutron fluence 2.8×10^{12} neutron/cm^2, γ-ray 3.1×10^{-1} Gy) at KURNS (thermal neutron flux 1.4×10^{9} neutron/cm^2/s), we carried out a cell proliferation assay (WST-1 assay) over 48 h and colony formation assay over 14 days (Fig. 5A, C, D). Fig. 5B shows the WST-1 assay results for U87 delta EGFR after 24 h and 48 h, following 1 MW neutron irradiation at KURNS for 15 min (thermal neutron fluence 1.1×10^{12} neutron/cm^2, γ-ray 2.5×10^{-1} Gy), or 30 min (thermal neutron fluence 2.4×10^{12} neutron/cm^2, γ-ray 5.5×10^{-1} Gy). No significant differences were observed for the control group for any radiation time (Fig. 5A). In contrast, the 100 μM A6K/1 mM BSH and 200 μM A6K/2 mM BSH groups showed inhibition of cell proliferation dependent on neutron radiation dose and irradiation time (Fig. 5A). The WST-1 assay results indicate an acute cell death reaction 48 h after the boron neutron reaction. In addition, the colony formation assay carried out 14 days after the boron neutron reaction showed late and slow cell reaction (Fig. 5C, D). The control groups were exposed to neutron irradiation without boron drug. The number of colonies formed in the control group showed little change with exposure time. However, the colony formation assay for the A6K/BSH complex groups—100 μM A6K/1 mM BSH and 200 μM A6K/2 mM BSH—showed survival ratios of 1, 0.78, 0.39, and 0.08 and 1, 0.27, 0.10, and 0.03, for 0, 5, 15, and 30 min neutron irradiation periods, respectively (Fig. 5C, D). The group treated with BSH only showed ratios of 1, 0.65, and 0.5 for 0, 5, and 15 min neutron irradiation periods. In the colony formation assay, the suppressive effect was clear for both A6K/BSH complex groups with thermal neutron irradiation dose escalation (Fig. 5D). Compared with the 2 mM BSH treated group, the A6K/BSH complex groups showed inhibition of cell proliferation following 15 min and 30 min neutron irradiation in both 24 h and 48 h WST-1 assays (Fig. 5B).

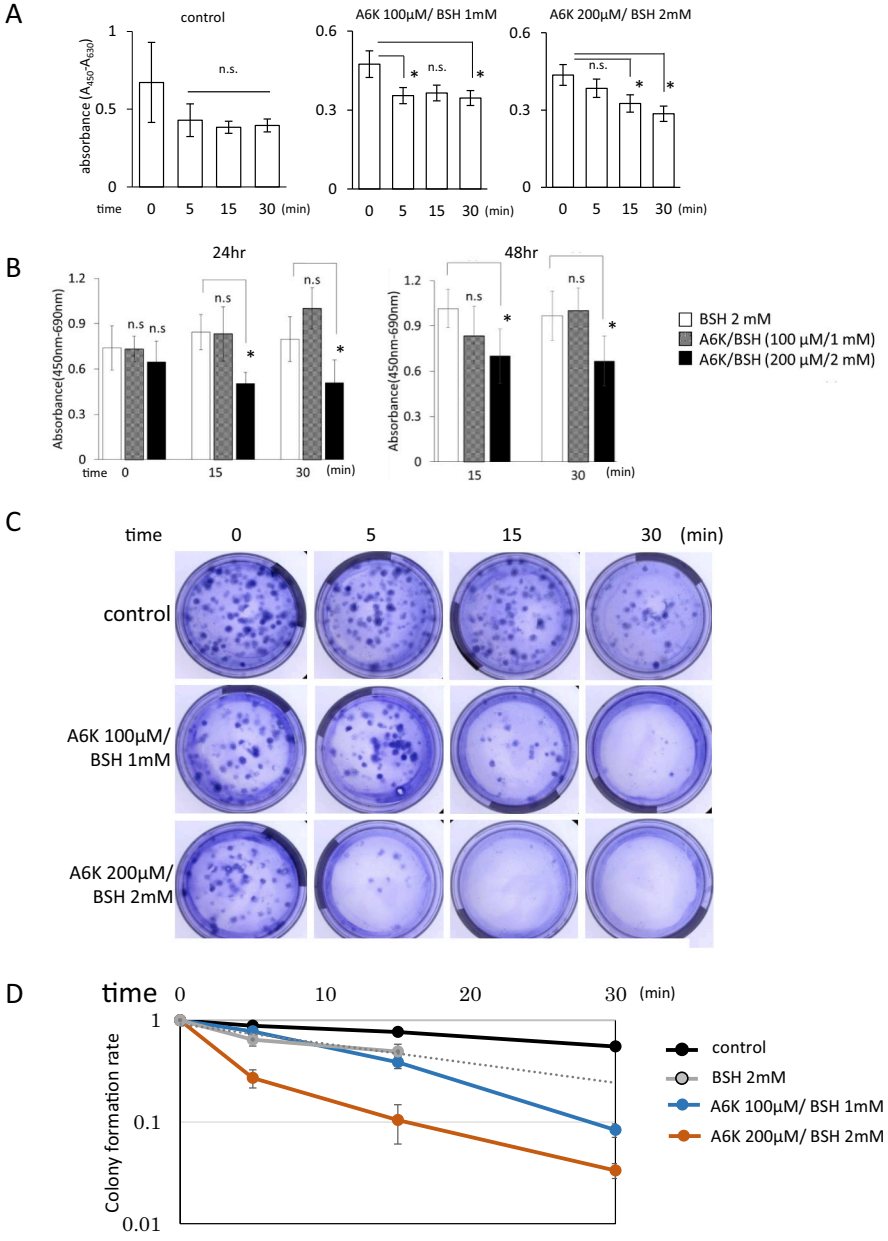

Fig. 5. The boron neutron reaction *in vitro* with low or high dose A6K/BSH complex in U87 delta EGFR cells analyzed at KURNS: (A)(B) Cell proliferation by WST-1 assay after 24 and 48 h incubation for different neutron irradiation times (1 MW; 0, 5, 15, and 30 min), y-axis shows the value of absorbance in the range 450–690 nm measured with an absorptiometer. (C)(D) U87 delta EGFR cell colony formation assay with CV staining after 14 days for different neutron irradiation times (black line: control group, gray line: 2 mM BSH, blue line: low dose 100 μM A6K/1 mM BSH, and orange line high dose 200 μM A6K/2 mM BSH, in each case n = 4). (For interpretation of the references to colour in this figure legend, the reader is referred to the web version of this article.)

4. Discussion

Numerous potential boron delivery systems based on macromolecular aggregates have been reported in the BNCT research field, particularly liposomes and water-in-oil-in-water (W/O/W) emulsions [20–23]. Small unilamellar liposomes composed of a pure synthetic phospholipid and cholesterol encapsulating water-soluble ionic boron compounds (B10H10(2-), B12H11SH2-, B20H17OH4-, B20H19(3-), B20H18(2-)); distearoylphosphatidylcholine (DSPC) liposomes and DSPC–PEG liposomes with nido-carborane lipid; and small, unilamellar BSH-encapsulating, transferrin (TF)-conjugated polyethyleneglycol liposomes (TF-PEG liposomes) as colon cancer and brain tumor targeting system have been reported [24–26]. However, several challenges relating to low toxicity with mass administration, drug stability of the encapsulated boron compounds, and tumor-specific accumulation, remain barriers to the practical application of boron drugs with macromolecular DDS for clinical BNCT [27].

Our peptide DDS concept is different to the conventional boron drug delivery systems previously described [19,28]. In the development of modern peptide chemistry, several short peptides have been found to exhibit various morphological structures and to be appropriate for use as drug delivery tools [29]. The lipid-like self-assembly of short peptides into nanotubes is a ubiquitous phenomenon. One of the leading lipid-like peptide nano-vesicle systems is the A6K nanotube [28,29]. The A6K peptide is an amphiphilic peptide that contains a cationic amino acid. In water, A6K easily forms luminal macaroni shapes, exposing lysine at the surface of the peptide nanotube [30]. The lipid-like self-assembling peptide A6K is therefore a suitable carrier for negatively charged drugs. The A6K drug delivery method is currently used for nucleic acid medicine and an A6K/siRNA complex has been investigated as a new drug against breast cancer at the National Cancer Center Japan [19,31,32].

A major advantage of the new A6K/BSH boron drug is the simple mixing of A6K peptide and BSH solution to make up the complex just before drug use without complicated drug adjustment steps [33]. In a recently published example focusing on the widely used drug BPA, poly

(vinyl alcohol) (PVA) was shown to readily form complexes with BPA through reversible boronate esters and the complex of PVA-BPA showed strong tumor accumulation in a mouse model [33]. This PVA-BPA complex demonstrates the clinical relevance of BNCT delivery systems whose preparation can be easily translated for practical use. The development of new boron agents for clinical application is expensive and time consuming. However, the A6K peptide delivery tool is in the clinical trial stage and BSH has been a BNCT clinical trial drug for malignant brain tumor treatment for a long time. Both drugs have been confirmed as safe and stable for clinical use. In this paper, A6K/BSH complex showed high tumor specific accumulation in IHC, high T/N ratio (2.5 time or more) and high boron concentration (20 ppm ^{10}B or more) in mouse brain tumor in PK study. The A6K/BSH complex is of course a new drug requiring preclinical testing; however, the barriers to its use may be lower based on the safety of its components.

In this work we chose an A6K/BSH mixture ratio of 1:10, therefore A6K peptide was added to BSH solution at 10% molar concentration and mixed gently by pipetting. The addition of an A6K supplement to a BSH solution to prepare a new boron drug is both innovative and simple in terms of drug design, and provides a different approach to those previously explored in the conventional boron DDS field. Because BSH is a negatively charged compound and A6K is a positively charged peptide, the two drugs easily formed a complex through electrostatic interaction [34]. Indeed, several studies have reported the mechanism of A6K/siRNA complex formation on the same principle. In the future, when there are potentially many negatively charged boron compounds, new boron complexes with A6K nanotubes can be investigated for intracellular transduction for BNCT.

The mechanism for A6K/BSH complex transduction into cells is thought to be endocytosis because many previous reports have found that A6K/siRNA enters the cell *via* endocytosis. The surfaces of A6K/material complexes have a positive charge, and the electrostatic interaction between the complex surface and the negatively charged cell membrane causes attachment of the drug to the cell before endocytosis [34]. Other DDS tools, such as liposomes, have several limitations in terms of the encapsulation of boron drugs inside the particles; however, the A6K/BSH system shows facile drug encapsulation [35]. This work has demonstrated that a new BSH compound—BSH supplemented with A6K peptide at 10 mol%—is a new potential candidate for the next generation of boron drugs. The precise mechanism for the cell uptake of the new boron complex requires further investigation. However, our experimental results demonstrate the potential clinical relevance of combining a peptide DDS with the boron drug BSH.

Grant support

This work was supported by a Grant-in-aid for Takeda Science Foundation, Nakatani Foundation for Advancement of Measuring Technologies in Biomedical Engineering, Scientific Research KAKENHI (18K07324 and 15K10333) from the Ministry of Education, Science, Sports, Takeda Science Foundation and Scientific. This research was funded by the Japan Agency for Medical Research and Development (AMED) (18072932) to A.F. We are grateful to 3-D Matrix, Ltd. for giving us A6K peptide for research use and a research grant for our future projects.

Acknowledgments

We are grateful to 3-D Matrix, Ltd. for giving us A6K peptide for research use and a research grant for our future projects. The U87 delta EGFR cell line was kindly provided by Prof. W. Cavenee and Dr. A. Mukasa at UCSD. The anti-BSH antibody was kindly provided by Prof. M. Kirihata at Osaka Prefectural University for immunocytochemistry and immunohistochemistry. The Boron ICP measurement was overseen by Dr. H. Nagare (Okayama University Faculty of Environmental Science and Technology). Ms. M. Furutani, Mr. H. Urata, and Ms. M. Tsukano (Central Research Laboratory, Okayama University Medical School) kindly assisted with the electron microscopy experiments. We thank Ms. A. Ueda for excellent technical assistance in our lab. We would like to thank the Institute of Plant Science and Resources (IPSR), Okayama University, Japan for assistance with the ICP-MS analysis. We thank Sarah Dodds, PhD, from Edanz Group (https://en-author-services.edanzgroup.com/ac) for editing a draft of this manuscript.

References

[1] R. Stupp, W.P. Mason, M.J. van den Bent, M. Weller, B. Fisher, M.J. Taphoorn, K. Belanger, A.A. Brandes, C. Marosi, U. Bogdahn, J. Curschmann, R.C. Janzer, S. K. Ludwin, T. Gorlia, A. Allgeier, D. Lacombe, J.G. Cairncross, Radiotherapy plus concomitant and adjuvant temozolomide for glioblastoma, N. Engl. J. Med. 352 (2005) 987–996.

[2] L.L. Muldoon, C. Soussain, K. Jahnke, C. Johanson, T. Siegal, Q.R. Smith, W. A. Hall, K. Hynynen, P.D. Senter, D.M. Peereboom, E.A. Neuwelt, Chemotherapy delivery issues in central nervous system malignancy: a reality check, J. Clin. Oncol. 25 (2007) 2295–2305.

[3] C.G. Rusthoven, M. Koshy, D.J. Sher, Radiation plus Temozolomide in patients with glioblastoma, N. Engl. J. Med. 376 (2017) 2195–2197.

[4] S. Kawabata, S. Miyatake, T. Kuroiwa, K. Yokoyama, A. Doi, K. Iida, S. Miyata, N. Nonoguchi, H. Michiue, M. Takahashi, T. Inomata, Y. Imahori, M. Kirihata, Y. Sakurai, A. Maruhashi, H. Kumada, K. Ono, Boron neutron capture therapy for newly diagnosed glioblastoma, J. Radiat. Res. 50 (2009) 515–560.

[5] S. Miyatake, S. Kawabata, K. Yokoyama, T. Kuroiwa, H. Michiue, Y. Sakurai, H. Kumada, M. Suzuki, A. Maruhashi, M. Kirihata, K. Ono, Survival benefit of boron neutron capture therapy for recurrent malignant gliomas, J. Neuro-Oncol. 91 (2009) 199–206.

[6] S. Kawabata, S. Miyatake, N. Nonoguchi, R. Hiramatsu, K. Iida, S. Miyata, K. Yokoyama, A. Doi, Y. Kuroda, T. Kuroiwa, H. Michiue, H. Kumada, M. Kirihata, Y. Imahori, A. Maruhashi, Y. Sakurai, M. Suzuki, S. Masunaga, K. Ono, Survival benefit from boron neutron capture therapy for the newly diagnosed glioblastoma patients, Appl. Radiat. Isot. 67 (75–8 Suppl) (2009) S15–S18.

[7] S. Miyatake, S. Kawabata, K. Yokoyama, T. Kuroiwa, H. Michiue, Y. Sakurai, H. Kumada, M. Suzuki, A. Maruhashi, M. Kirihata, K. Ono, Survival benefit of boron neutron capture therapy for recurrent malignant gliomas, Appl. Radiat. Isot. 67 (75–8 Suppl) (2009) S22–S24.

[8] H. Michiue, Y. Sakurai, N. Kondo, M. Kitamatsu, F. Bin, K. Nakajima, Y. Hirota, S. Kawabata, T. Nishiki, I. Ohmori, K. Tomizawa, S. Miyatake, K. Ono, H. Matsui, The acceleration of boron neutron capture therapy using multi-linked (BSH) fused cell-penetrating peptide, Biomaterials 35 (2014) 33405–33965.

[9] Y. Iguchi, H. Michiue, M. Kitamatsu, Y. Hayashi, F. Takenaka, T. Nishiki, H. Matsui, Tumor-specific delivery of BSH-3R for boron neutron capture therapy and positron emission tomography imaging in a mouse brain tumor model, Biomaterials 56 (2015) 105–107.

[10] M. Suzuki, Boron neutron capture therapy (BNCT): a unique role in radiotherapy with a view to entering the accelerator-based BNCT era, Int. J. Clin. Oncol. 25 (2020) 43–50.

[11] R.F. Barth, Z. Zhang, T. Liu, A realistic appraisal of boron neutron capture therapy as a cancer treatment modality, Cancer Commun. (Lond.) 38 (2018) 36.

[12] P. Wongthai, K. Hagiwara, Y. Miyoshi, P. Wiriyasermkul, L. Wei, R. Ohgaki, I. Kato, K. Hamase, S. Nagamori, Y. Kanai, Boronophenylalanine, a boron delivery agent for boron neutron capture therapy, is transported by ATB0,+, LAT1 and LAT2, Cancer Sci. 106 (3) (2015) 2786–2795.

[13] E. Sato, T. Yamamoto, N. Shikano, M. Ogura, K. Nakai, F. Yoshida, Y. Uemae, T. Takada, T. Isobe, A. Matsumura, Intracellular boron accumulation in CHO-K1 cells using amino acid transport control, Appl. Radiat. Isot. 88 (2014) 103–995.

[14] A. Detta, G.S. Cruickshank, L-amino acid transporter-1 and boronophenylalanine-based boron neutron capture therapy of human brain tumors, Cancer Res. 69 (5) (2009) 21232–21265.

[15] K. Sköld, T. Gorlia, L. Pellettieri, V. Giusti, B. H-Stenstam, J.W. Hopewell, Boron neutron capture therapy for newly diagnosed glioblastoma multiforme: an assessment of clinical potential, Br. J. Radiol. 83 (991) (2010) 5603–5965.

[16] S. Miyatake, S. Kawabata, R. Hiramatsu, T. Kuroiwa, M. Suzuki, N. Kondo, K. Ono, Boron neutron capture therapy for malignant brain tumors, Neurol. Med. Chir. (Tokyo) 56 (7) (2016) 3615–3671.

[17] H. Nakamura, Boron lipid-based liposomal boron delivery system for neutron capture therapy: recent development and future perspective, Future Med. Chem. 5 (6) (2013) 7130–7155.

[18] Y. Chen, C. Tang, J. Zhang, M. Gong, B. Su, F. Qiu, Self-assembling surfactant-like peptide A6K as potential delivery system for hydrophobic drugs, Int. J. Nanomed. 10 (2015) 8458–8475.

[19] D. Yoshida, K. Kim, I. Takumi, F. Yamaguchi, K. Adachi, A. Teramoto, A transfection method for short interfering RNA with the lipid-like self-assembling nanotube, A6K, Med. Mol. Morphol. 46 (2013) 865–891.

[20] H. Nakamura, Liposomal boron delivery for neutron capture therapy, Methods Enzymol. 465 (2009) 1208–1795.

[21] M. Ueda, K. Ashizawa, K. Sugikawa, K. Koumoto, T. Nagasaki, A. Ikeda, Lipid-membrane-incorporated arylboronate esters as agents for boron neutron capture therapy, Org. Biomol. Chem. 15 (7) (2017) 15655–15669.

[22] Z. Gao, Y. Horiguchi, K. Nakai, A. Matsumura, M. Suzuki, K. Ono, Y. Nagasaki, Use of boron cluster-containing redox nanoparticles with ROS scavenging ability, Biomaterials 104 (2016) 2012–2015.
[23] H. Azuma, Y. Aizawa, N. Higashitani, T. Tsumori, A. Kojima-Yuasa, I. Matsui-Yuasa, T. Nagasaki, Biological activity of water-soluble inclusion complexes of 1'-acetoxychavicol acetate with cyclodextrins, Bioorg. Med. Chem. 19 (12) (2011) 38555–38563.
[24] Y. Ito, Y. Kimura, T. Shimahara, Y. Ariyoshi, M. Shimahara, S. Miyatake, S. Kawabata, S. Kasaoka, K. Ono, Disposition of TF-PEG-liposome-BSH in tumor-bearing mice, Appl. Radiat. Isot. 67 (7–8 Suppl) (2009) S1095–S1096.
[25] A. Doi, S. Kawabata, K. Iida, K. Yokoyama, Y. Kajimoto, T. Kuroiwa, T. Shirakawa, M. Kirihata, S. Kasaoka, K. Maruyama, H. Kumada, Y. Sakurai, S. Masunaga, K. Ono, S. Miyatake, Tumor-specific targeting of sodium borocaptate (BSH) to malignant glioma by transferrin-PEG liposomes: a modality for boron neutron capture therapy, J. Neuro-Oncol. 87 (3) (2008) 2875–2894.
[26] B. Feng, K. Tomizawa, H. Michiue, X. Han, S. Miyatake, H. Matsui, Development of a bifunctional immunoliposome system for combined drug delivery and imaging in vivo, Biomaterials 31 (14) (2010) 41345–41395.
[27] B. Feng, K. Tomizawa, H. Michiue, S. Miyatake, X. Han, A. Fujimura, M. Seno, M. Kirihata, H. Matsui, Delivery of sodium borocaptate to glioma cells using immunoliposome conjugated with anti-EGFR antibodies by ZZ-His, Biomaterials 30 (9) (2009) 17455–17465.
[28] Y. Chen, C. Tang, J. Zhang, M. Gong, B. Su, F. Qiu, Self-assembling surfactant-like peptide A6K as potential delivery system for hydrophobic drugs, Int. J. Nanomedicine 10 (2015) 8458–8475.
[29] D.G. Fatouros, D.A. Lamprou, A.J. Urquhart, S.N. Yannopoulos, I.S. Vizirianakis, S. Zhang, S. Koutsopoulos, Lipid-like self-assembling peptide nanovesicles for drug delivery, ACS Appl. Mater. Interfaces 6 (2014) 81845–81849.
[30] A. Nagai, Y. Nagai, H. Qu, S. Zhang, Dynamic behaviors of lipid-like self-assembling peptide A6D and A6K nanotubes, J. Nanosci. Nanotechnol. 7 (7) (2007) 22452–22465.
[31] K. Honma, K. Iwao-Koizumi, F. Takeshita, Y. Yamamoto, T. Yoshida, K. Nishio, S. Nagahara, K. Kato, T. Ochiya, RPN2 gene confers docetaxel resistance in breast cancer, Nat. Med. 14 (9) (2008) 939–948.
[32] N. Habibi, N. Kamaly, A. Memic, H. Shafiee, Self-assembled peptide-based nanostructures: Smart nanomaterials toward targeted drug delivery, Nano Today 11 (1) (2016) 415–460.
[33] T. Nomoto, Y. Inoue, Y. Yao, M. Suzuki, K. Kanamori, H. Takemoto, M. Matsui, K. Tomoda, N. Nishiyama, Poly(vinyl alcohol) boosting therapeutic potential of p-boronophenylalanine in neutron capture therapy by modulating metabolism, Sci. Adv. 6 (4) (2020) (eaaz1722).
[34] A.L. Schachner-Nedherer, O. Werzer, K. Kornmueller, R. Prassl, A. Zimmer, Biological activity of miRNA-27a using peptide-based drug delivery systems, Int. J. Nanomedicine 14 (2019) 77808–77955.
[35] M. Shirakawa, T. Yamamto, K. Nakai, K. Aburai, S. Kawatobi, T. Tsurubuchi, Y. Yamamoto, Y. Yokoyama, H. Okuno, A. Matsumura, Synthesis and evaluation of a novel liposome containing BPA-peptide conjugate for BNCT, Appl. Radiat. Isot. 67 (75–8 Suppl) (2009) S885–S890.